Supplementary Material (ESI) for Soft Matter

Supporting Information

Helical nano-structures self-assembled from dimethylaminoethyloxy-containing unsymmetrical octakis-substituted phthalocyanine derivatives

Pan Ma, Zhaopin Bai, Yingning Gao, Jinglan Kan, Yongzhong Bian and Jianzhuang Jiang*

Synthesis of unsymmetrical znic 2,3,9,10,16,17,23-heptakis(butyloxy)-24-mono(dimethylaminoethyloxy)-phthalocya nine Zn{Pc(OC_4H_9)$_7$[$OC_2H_4N(CH_3)_2$]} (2). $Zn(OAc)_2{\cdot}2H_2O$ (20 mg, 0.09 mmol), H_2{Pc(OC_4H_9)$_7$[$OC_2H_4N(CH_3)_2$]} (33 mg, 0.03 mmol) in 3 ml DMF was stirred for 4 h at 140°C. The solution containing the reaction mixture was concentrated and then chromatographed on a silica gel column with $CHCl_3$ as eluent. Repeated chromatography followed by recrystallization from $CHCl_3$ and methanol gave pure target compound Zn{Pc(OC_4H_9)$_7$[$OC_2H_4N(CH_3)_2$]} as a reddish purple powder (29 mg, 85%). MS (MALDI-TOF) an isotopic cluster peaking at ***m/z*** 1167.7 (Calc. for M^+ 1167.5). Anal. Calc. for $ZnC_{64}H_{81}N_9O_8$: C, 65.71%; H, 6.98%; N, 10.78%. Found: C, 65.38%; H, 6.18%; N, 10.90%. UV-Vis ($CHCl_3$) [λ_{max}/nm (logε)] 366 (4.53), 613(4.08), 681 (4.76), 692(4.84); UV-Vis ($CHCl_3$ + pyridine) [λ_{max}/nm (logε)] 362 (4.52), 613(4.07), 680(4.89). ^{1}H NMR[$CDCl_3$/pyridine-d5 (99:1), 300 MHz]: 8.93-8.89 **(Ar-*H*)**, 4.568 (t, O***CH$_2$***), 2.98 [t, OCH_2***CH_2***$N(CH_3)_2$], 2.43[s, OCH_2CH_2N(***CH_3***)$_2$], 2.05(m, OCH_2***CH_2***CH_2CH_3), 1.68-1.70 (m, OCH_2CH_2***CH_2***CH_3), 1.06-1.11 (t, $OCH_2CH_2CH_2$***CH_3***).

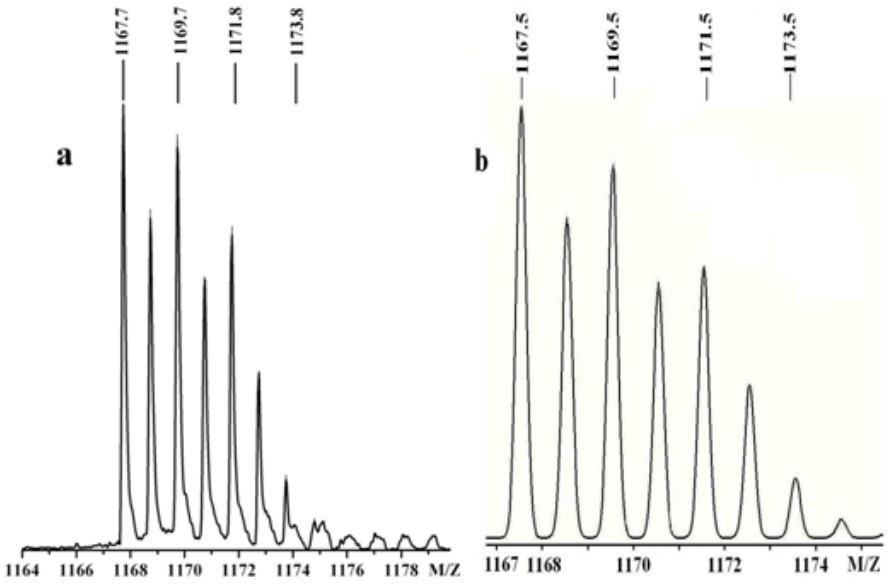

Fig. S1. Experimental (a) and simulated isotopic patterns (b) for molecular ion of phthalocyaninato zinc complex Zn{Pc(OC_4H_9)$_7$[$OC_2H_4N(CH_3)_2$]} (**2**).

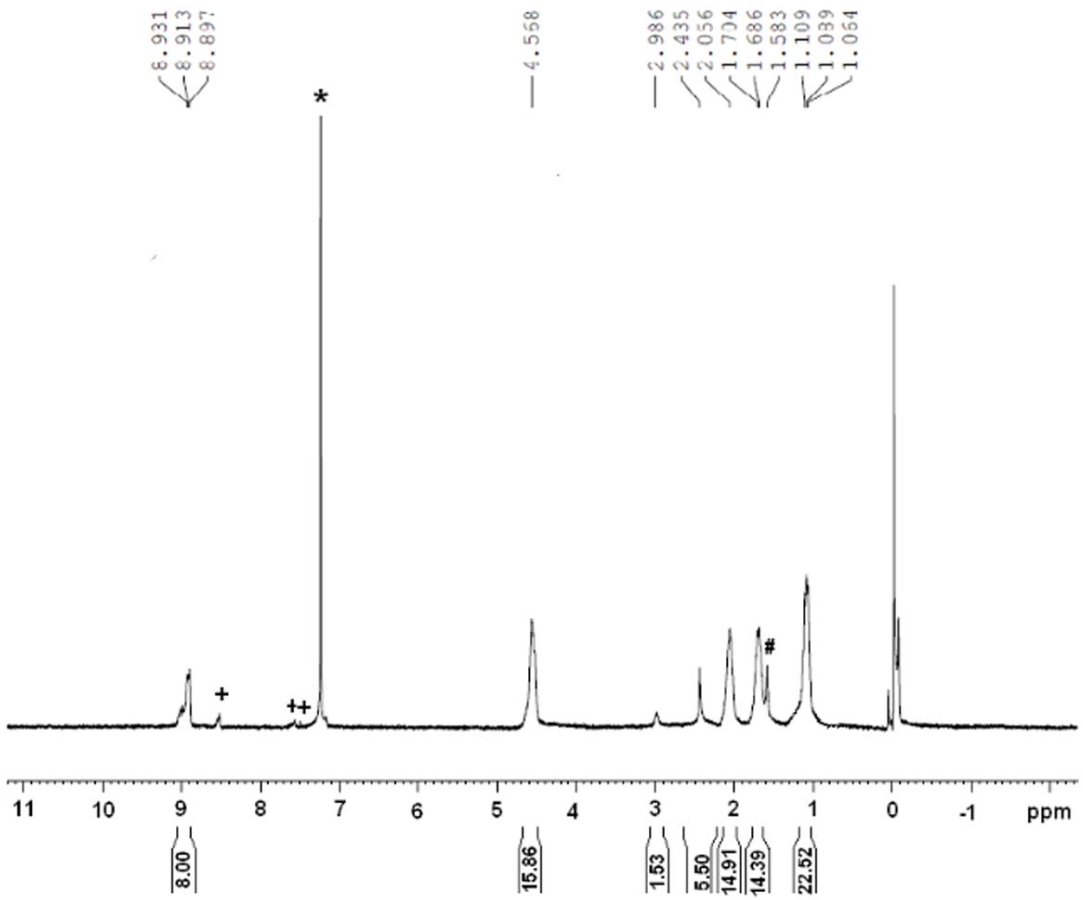

Fig. S2. The ^{1}H NMR spectrum of $Zn\{Pc(OC_4H_9)_7[OC_2H_4N(CH_3)_2]\}$ (**2**) in $CDCl_3$/pyridine-d_5 (99:1). The signals due to pyridine-d_5, residue $CHCl_3$ and water are denoted as $^{+}$, *, and $^{\#}$, respectively.

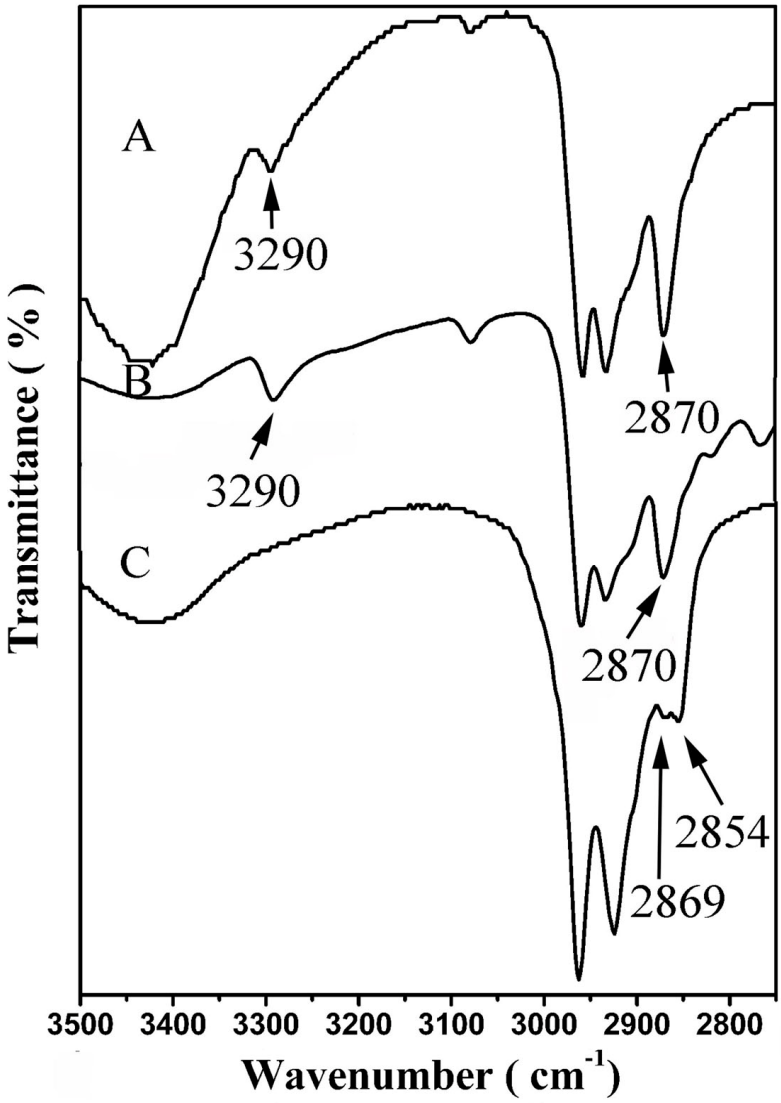

Fig. S3. IR spectra of $H_2Pc(OC_4H_9)_8$ (A), $H_2\{Pc(OC_4H_9)_7[OC_2H_4N(CH_3)_2]\}$ (**1**) (B), and the aggregates of **1** formed in methanol (C) in the region 2750-3500 cm^{-1} with 2 cm^{-1} resolution.

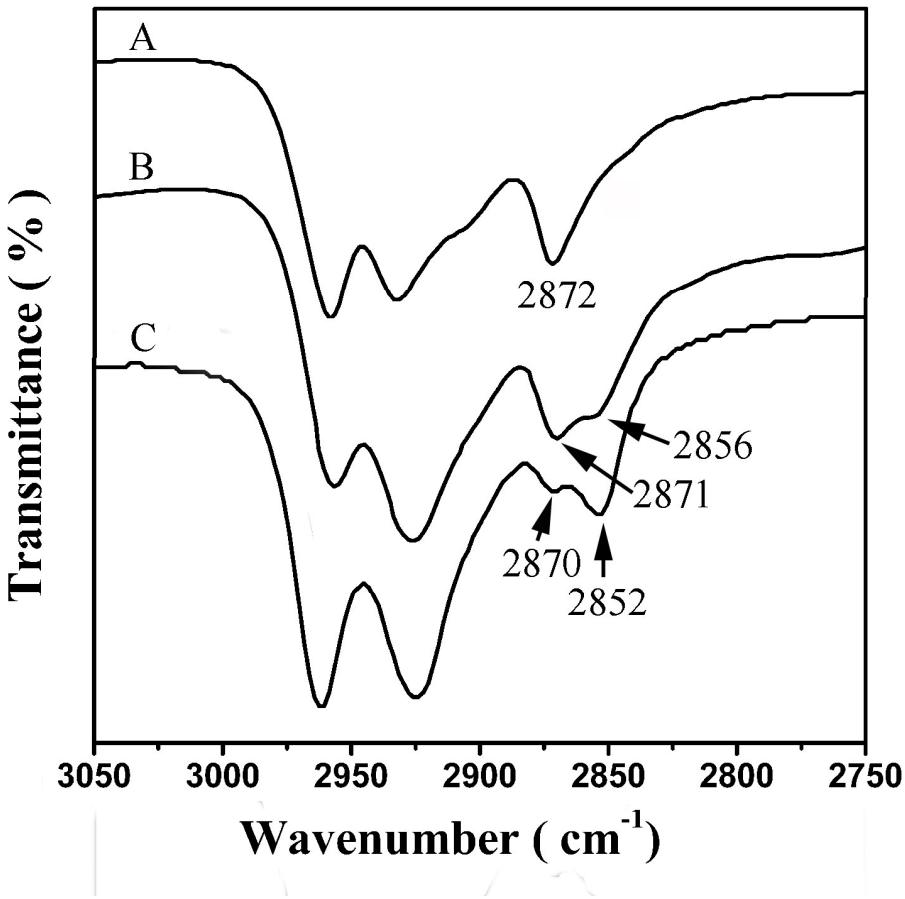

Fig. S4. IR spectra of compound $Zn\{Pc(OC_4H_9)_8$ (A), $Zn\{Pc(OC_4H_9)_7[OC_2H_4N(CH_3)_2]\}$ (**2**) (B), and the aggregates of **2** formed in methanol (C) in the region 2750-3050 cm^{-1} with 2 cm^{-1} resolution.

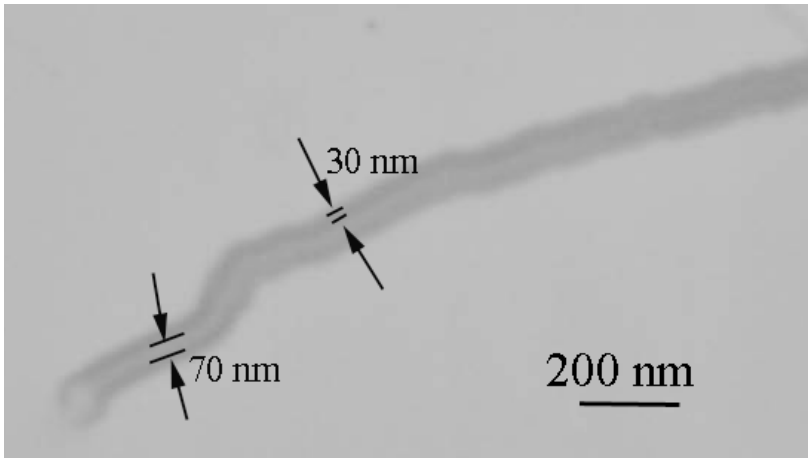

Fig. S5. TEM image of tubular superstructure of $H_2\{Pc(OC_4H_9)_7[OC_2H_4N(CH_3)_2]\}$ (**1**).

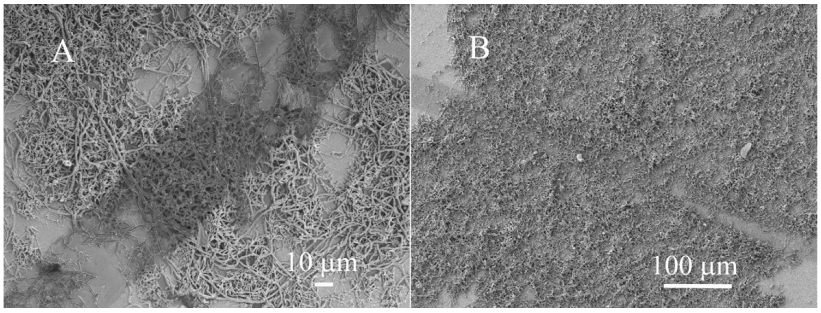

Figure S6. SEM images of the two-electrode device fabricated on SiO_2: (A) nanostructures of $H_2\{Pc(OC_4H_9)_7[OC_2H_4N(CH_3)_2]\}$ (**1**), (B) nanowire bundles of $Zn\{Pc(OC_4H_9)_7[OC_2H_4N(CH_3)_2]\}$(**2**).

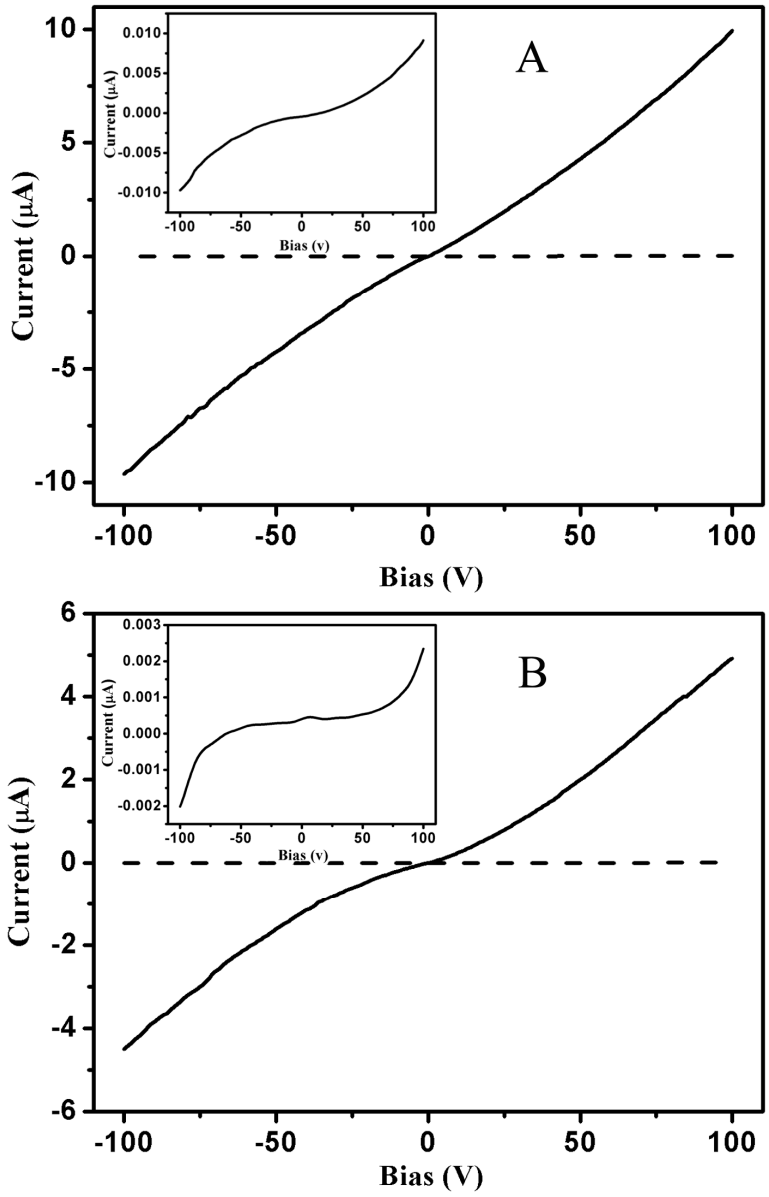

Figure S7. *I-V* curves measured on $H_2\{Pc(OC_4H_9)_7[OC_2H_4N(CH_3)_2]\}$ drop-casting film (A) and $Zn\{Pc(OC_4H_9)_7[OC_2H_4N(CH_3)_2]\}$ drop-casting film (B): undoped (dash line), doped with iodine vapor (solid line). The inset is the *I-V* curve of undoped drop-casting film from –100 to 100V.

Table S1. Electronic absorption data for compounds $H_2\{Pc(OC_4H_9)_7[OC_2H_4N(CH_3)_2]\}$ (**1**) and $Zn\{Pc(OC_4H_9)_7[OC_2H_4N(CH_3)_2]\}$ (**2**) dissolved in $CHCl_3$ and their self-assemblies dispersed in methanol.

Compound	λmax / nm	
	$CHCl_3$	methanol
1	349, 426, 603, 646, 665, 702	330, 403, 609
2	362, 421, 680, 692	357, 409, 615